

Anisotropy of crack and dislocation formation in GaAs

Ingmar Ratschinski^{*1}, Frank Heyroth¹, Wolfgang Fränzel², and Hartmut S. Leipner^{**1}

¹ Interdisziplinäres Zentrum für Materialwissenschaften, Martin-Luther-Universität Halle-Wittenberg, Heinrich-Damerow-Straße 4, 06210 Halle, Germany

² Institut für Physik, Martin-Luther-Universität Halle-Wittenberg, Friedemann-Bach-Platz 6, 06108 Halle, Germany

Received 17 September 2008, revised 19 December 2008, accepted 14 April 2009

Published online 17 June 2009

PACS 61.72.Ff, 61.72.Lk, 61.72.uj, 62.20.mt

* Corresponding author: e-mail ratschinski@web.de, Phone: +49 345 5528 485, Fax: +49 345 5527 390

** e-mail hartmut.leipner@cmat.uni-halle.de, Phone: +49 345 5528 473, Fax: +49 345 5527 390

The dependence of cracking at Vickers indentations in (100) GaAs was investigated for different dopings by electron microscopy. Depending on the load, the formation of cracks was studied. In semiinsulating carbon-doped GaAs, a clear anisotropy in the cracking pattern exists with cracks running prefer-

entially along the $\pm [011]$ directions. In contrast, in n-type as well as in p-type GaAs little or no anisotropic crack pattern can be recognized. The formation and propagation of cracks does not correlate with the formation of the dislocation rosette.

© 2009 WILEY-VCH Verlag GmbH & Co. KGaA, Weinheim

1 Introduction GaAs is a III-V compound semiconductor crystallizing in the zinc blende structure. Due to the missing inversion center, $\{100\}$ and $\{111\}$ planes are polar, i.e. they are terminated by only one sort of atoms. This is the reason for the different mobility of α and β dislocations. The $\{110\}$ planes are nonpolar and form the cleavage planes in GaAs.

In the zinc blende structure, screw dislocations as well as 60° α and β dislocations having a Burgers vector of $a/2\langle 110 \rangle$ and different velocities v_s , v_α , v_β , dominate. The velocity depends on the type of dislocation, the doping, the temperature and the shear stress. It can be increased by illumination and electron beam irradiation. In undoped and n-type GaAs (e.g. tellurium or silicon doping), $v_\alpha > v_\beta > v_s$. In highly p-doped GaAs (zinc doping) $v_\beta > v_s > v_\alpha$ [1]. The movement of α , β and screw dislocations takes place in the glide set. The elastic energy of a 60° dislocation can be reduced by the dissociation into a 30° and a 90° dislocation. Between the two partial dislocations, a stacking fault exists. According to Lu and Cockayne [2], the dislocations move in the dissociated state.

The classic model of crack nucleation is the pile-up of dislocations at the intersection of two different glide planes [3]. Dislocations can dissociate on the (111) plane

$$\mathbf{b}_1 \rightarrow \mathbf{b}_2 + \mathbf{b}_3: \frac{a}{2}[\bar{1}10] \rightarrow \frac{a}{6}[2\bar{1}1] + \frac{a}{6}[\bar{1}2\bar{1}] \quad (1)$$

and the $(\bar{1}11)$ plane:

$$\mathbf{b}_4 \rightarrow \mathbf{b}_5 + \mathbf{b}_6: \frac{a}{2}[101] \rightarrow \frac{a}{6}[1\bar{1}2] + \frac{a}{6}[211] \quad (2)$$

The Burgers vectors of the involved dislocations are \mathbf{b}_i , $i = 1 \dots 7$. The partial dislocations \mathbf{b}_3 and \mathbf{b}_5 attract each other and can react at the intersection line of their glide planes:

$$\mathbf{b}_3 + \mathbf{b}_5 \rightarrow \mathbf{b}_7: \frac{a}{6}[\bar{1}2\bar{1}] + \frac{a}{6}[1\bar{1}2] \rightarrow \frac{a}{6}[011] \quad (3)$$

The new partial dislocation, called Lomer-Cottrell dislocation, is relatively stable. It is bonded by two stacking faults located in two different planes. Cracks can be nucleated by a dislocation pile-up at Lomer-Cottrell barriers. The size of a crack nucleus increases with the number of piled up dislocations, and the crack opening force increases with the mobility of the dislocations involved. A higher velocity of dislocations should lead to a higher opening force [4]. That would lead to the assumption of a higher formation probability of A-cracks (cracks resulting from the interaction of α dislocations) in undoped and n-type GaAs and of B-cracks (cracks resulting from the interaction of β dislocations) in highly p-doped GaAs.

The crack propagation can be suppressed by the dissipation of energy due to the movement of dislocations or the comprehensive stress due to the interaction of disloca-

tions [5]. According to Fujita et al. [4], dislocation emission at the crack could shield the stress field intensity at the crack tip and would suppress the crack propagation. Another model is the evolution of an atomically sharp crack in the cleavage plane and its propagation by kink-pair formation. Hence, the anisotropy of crack formation would be an effect of differences in kink-pair formation for different crack orientations (3D lattice trapping) [6, 7].

2 Experimental The materials investigated were (100) GaAs wafers produced by Freiberger Compound Materials doped with carbon ($[C] \approx 6.2 \times 10^{15} \text{ cm}^{-3}$), silicon ($[Si] \approx 1.85 \times 10^{18} \text{ cm}^{-3}$), tellurium ($[Te] = 1.4 \dots 3.5 \times 10^{17} \text{ cm}^{-3}$) or zinc ($[Zn] = 9.8 \times 10^{18} \text{ cm}^{-3}$). Vickers indentations were performed using a Hanemann mhp 100 micro hardness tester at room temperature. For each wafer, sets of 10 Vickers indentations with loads of 0.02 N, 0.05 N, 0.10 N, 0.25 N, 0.5 N and 1.0 N were performed. The indenter diagonals were oriented in $\langle 011 \rangle$ directions. The dwell time was 3 s and both the loading rate and the unloading rate were 125 mN per second for $F > 0.05 \text{ N}$ and approx. 1 second for $F \leq 0.05 \text{ N}$.

The distinction of $[011]$ and $[0\bar{1}1]$ directions has been made according to the orientation of major and minor wafer flats, provided by the wafer manufacturer.

The cracks were observed by scanning electron microscopy (SEM) using a Philips ESEM XL 30 FEG. The samples were imaged with secondary electrons (SE) at acceleration voltages of 2 or 5 kV. Slip lines were investigated with SEM and atomic force microscopy (AFM) using a Pacific Nanotechnology Nano-RTM. The dislocations were observed by cathodoluminescence (CL) imaging and transmission electron microscopy (TEM). The CL investigations were performed in a JEOL JSM 6400 at an acceleration voltage of 8 kV. The intensity of the light was recorded with a Hamamatsu R2228 photomultiplier using the entire spectra of emitted light (panchromatic contrast). For TEM investigations, a JEOL JEM 4000 FX was used at an acceleration voltage of 400 kV. For TEM preparation, indented samples were drilled out with an ultrasonic driller and cleaned in acetone and ethanol. The back side of the samples were grinded and dimpled mechanically. The samples were thinned by argon ions to a final thickness of approximately 0.7 μm in the region of the indentations using a Gatan precision ion polishing system model 691.

3 Crack formation around Vickers indentations

3.1 Characteristics of crack patterns

If the indenter diagonals are oriented in $\langle 110 \rangle$ directions, the crack patterns around Vickers indentations on the (100) surface have the following characteristics:

- Cracks occur along $\langle 011 \rangle$ directions at the indenter corners ($\langle 011 \rangle$ -cracks).
- The material beneath the $\langle 011 \rangle$ -cracks is cleaved along $\{011\}$ planes.

- Additional cracks occur at the edges of the indentation. They are not strictly crystallographically oriented ($\langle 001 \rangle$ -cracks).
- If a $\langle 011 \rangle$ -crack is absent, the $\langle 001 \rangle$ -cracks are longer and bent into the direction of the absent $\langle 011 \rangle$ -crack.
- Slip lines occur parallel to the $\langle 011 \rangle$ directions.
- The number of cracks rises with increasing load.

These results are in agreement with the results of Bergner et al. [8, 9]. Figure 1a shows a fully developed crack pattern and Fig. 1b a crack pattern with missing $\langle 011 \rangle$ -cracks in $\pm [0\bar{1}1]$ directions.

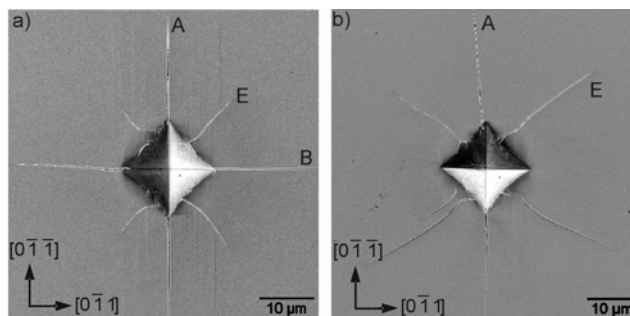


Figure 1 SE images of Vickers indentation in (100) GaAs:Te (load 1.0 N). Fully developed crack pattern (a) and missing cracks along the $\pm [0\bar{1}1]$ directions (b).

In the evaluation of the crack formation, $\langle 011 \rangle$ -cracks generated at the indenter corners and propagating in $\pm [011]$ directions are called A-cracks, corresponding to the direction of α dislocations, and $\langle 011 \rangle$ -cracks in $\pm [0\bar{1}1]$ directions (direction of β dislocations) are named B-cracks. Other cracks occur at the edge of the indentation. They are called E-cracks. Cracks are considered as A- or B-cracks, if the angle between the crack tip and the indentation diagonal is less than 10° . Otherwise, these cracks are counted as E-cracks. If the crack length outside the indentation is less than a third of the indentation diagonal, it is counted as crack seed. The number of A- and B-cracks per corner and the number of E-cracks per edge (crack numbers n_A , n_B , n_E) are used to investigate the crack formation (Figs. 2, 4, 5, 6). The statistic error is displayed as error bars. In Fig. 1a, the crack numbers n_A , n_B , n_E are equal to 1. In Fig. 1b, $n_A = 1$, $n_B = 0$, $n_E = 1.25$.

3.2 The influence of doping on crack formation

In carbon-doped GaAs, the crack numbers rise with increasing load (Fig. 2). The number of A-cracks n_A rises significantly in the range from 0.05 N to 0.1 N. n_A is equal to 1 for all loads from 0.25 N to 1.0 N. The crack numbers n_B and n_E are almost zero for loads less than 0.5 N and rises up to 0.6 and 0.7 at 1.0 N. Slip lines are found only in $\pm [011]$ directions. In carbon-doped GaAs, a distinct anisotropic crack formation exists between A-cracks and B-cracks. At loads of 0.1 N and 0.25 N A-cracks appear almost exclusively.

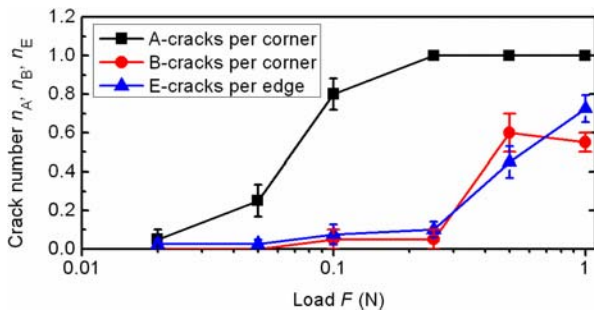


Figure 2 Crack formation in GaAs:C. Distinct anisotropic crack formation appears for A-cracks and B-cracks.

Figure 3 shows the most frequent crack patterns to illustrate the crack formation from Fig. 2. The load of the indentations and the frequency of the crack pattern are indicated at the top of the pictures.

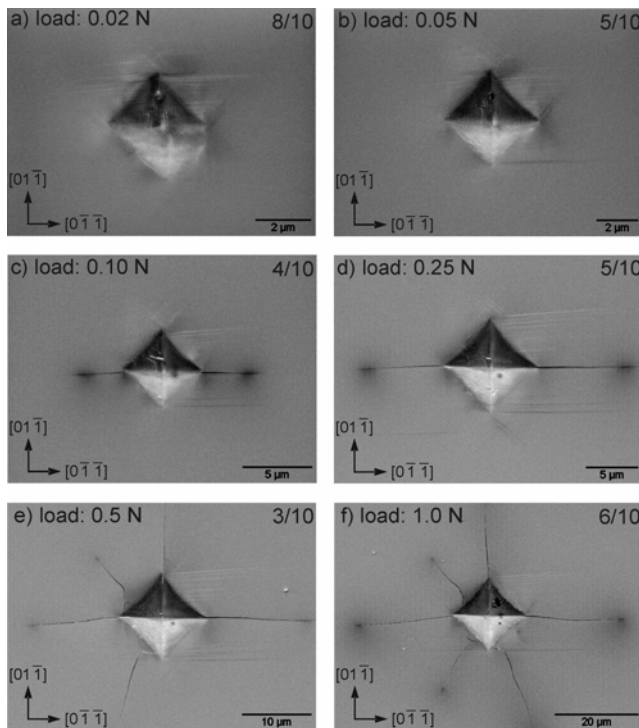


Figure 3 SE images of the most frequent crack patterns in GaAs:C. On the upper right corner, the frequency of the crack pattern out of 10 attempts is shown. a), b) At low loads, no cracks occur. c), d) Due to the anisotropic crack formation, mainly A-cracks appear. At higher loads, B-cracks and E-cracks occur (e). The number of E-cracks rises with increasing load (f).

In tellurium-doped GaAs, the crack numbers n_A and n_E are comparable (Fig. 4). Except for a load of 0.1 N, n_B is lower than the other crack numbers. It is thus concluded that in tellurium-doped GaAs, a slight anisotropy in crack formation may exist. The slip lines run parallel to the $\pm [011]$ directions.

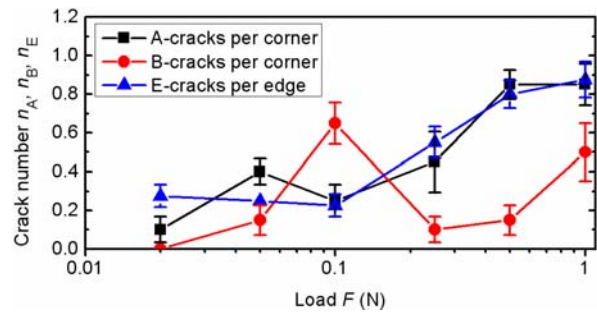


Figure 4 Crack formation in GaAs:Te.

In silicon-doped GaAs, the number of A-cracks is almost constant for loads in the range from 0.02 N to 0.25 N (Fig. 5). For higher loads, it increases lightly. The number of B-cracks is nearly constant except for a load of 0.02 N and 0.25 N. The number of E-cracks rises with increasing load up to 1.1 at 1.0 N, i.e. there is in average more than one crack per edge. An anisotropy of crack formation barely exists. The slip lines run in $\pm [011]$ directions.

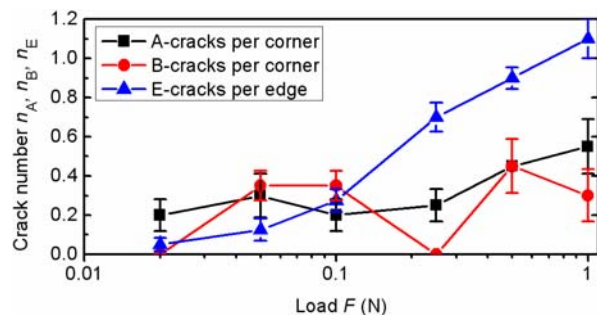


Figure 5 Crack formation in GaAs:Si.

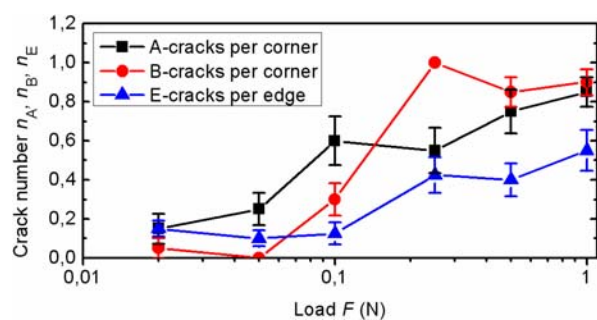


Figure 6 Crack formation in GaAs:Zn.

In zinc-doped GaAs, the crack numbers rise with increasing load (Fig. 6). At loads up to 0.1 N, n_A is higher than n_B , but in the range from 0.25 N to 1.0 N, n_A is lower. At a load in the range from 0.1 N to 1.0 N, n_E is lower than the other crack numbers. The slip lines run parallel to the $\pm [0\bar{1}1]$ directions. So, their orientation turns by 90° in comparison to the other materials. A low anisotropy in

crack formation in dependence on the load might be concluded.

4 Dislocation formation

4.1 CL investigations In GaAs, dislocations are centers of non-radiative recombination. At cracks total reflection occurs. Hence, dislocations and cracks appear dark in CL images (Fig. 7).

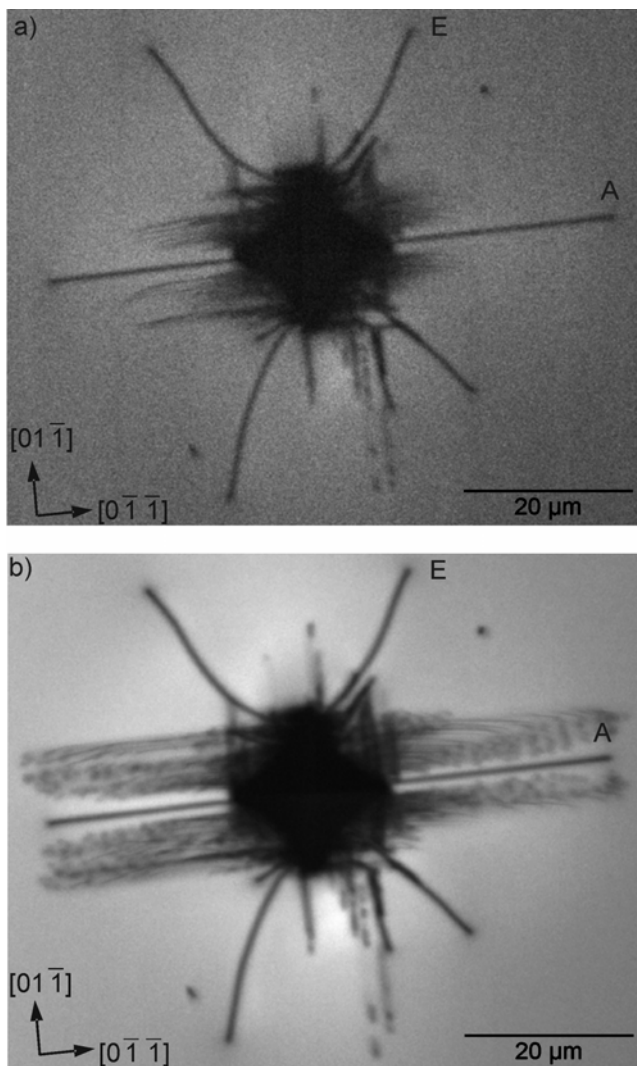


Figure 7 CL images of a Vickers indentation on GaAs:Si, load 1.0 N: movement of dislocations due to electron beam irradiation. a) First picture recording, beam current: $I = 1.25$ nA. b) Dislocations after electron beam irradiation. Irradiation and picture recording at a beam current of $I = 20.3$ nA.

Figure 7 shows the dislocation arrangement around a Vickers indentation in silicon-doped GaAs. In the CL pictures, the dislocation loops running parallel to the surface can be well recognized. Near the crack tips, there are no dislocations visible in Fig. 7a. For this reason, surface par-

allel dislocation half loops do not participate in the crack propagation. The dislocations move due to electron beam irradiation in the stress field of the indentation. Figure 7b shows the final dislocation arrangement. In this case, the dislocations in $\pm [011]$ directions extend to the end of the cracks.

4.2 TEM investigations Vickers indentations were investigated in TEM plane view. Figure 8 shows eight arms of dislocations, directed in different $\langle 110 \rangle$ directions. The arrangement of dislocations after indentations on a (100) surface of GaAs is in agreement with the glide prism model of Warren et al. [5]. Four arms are parallel to the surface, and the other arms are directed into the crystal. Each arm consists of two branches. At the corners of the indentation, dislocation half loops directed into the crystal cut each other. Deeper segments of the dislocation half loops directed into the crystal were cut during the TEM preparation by thinning the sample from the backside.

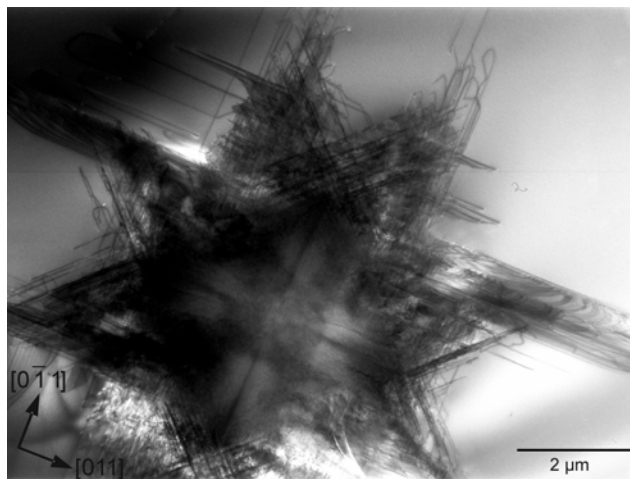


Figure 8 400 kV multiple-beam bright-field TEM image of dislocations around a Vickers indentation in GaAs:C, load: 100 mN.

A-cracks were observed to emanate from the corner of the indentation in a region having a high density of dislocation half loops directed into the crystal Fig. 9). The crack passes through the region between two surface parallel dislocation branches without interaction. Sometimes, close to the crack and at the crack tip, dislocations may occur. They may have suppressed further crack propagation as reported by Fujita et al. [4]. At indentations on (100) surfaces, the formation of Lomer-Cottrell dislocations is expected predominantly beneath the indentation. In this region, no single dislocations could be resolved in TEM samples in plane view. There are almost no surface parallel dislocations at the corners of the indentation (Figs. 8, 9, 10). It seems therefore to be unlikely that these dislocations are involved in formation of A-cracks and B-cracks.

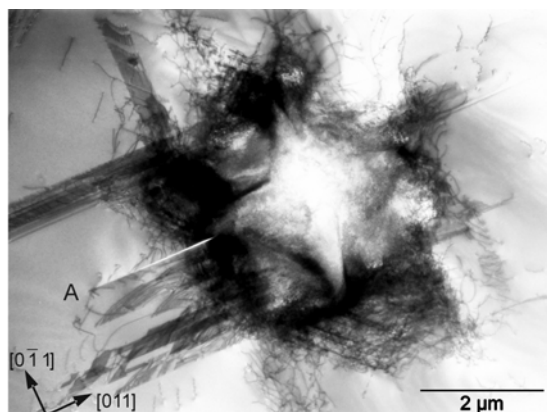


Figure 9 Multiple-beam bright-field TEM image: A-crack at a Vickers indentation in GaAs:C, load: 0.04 N.

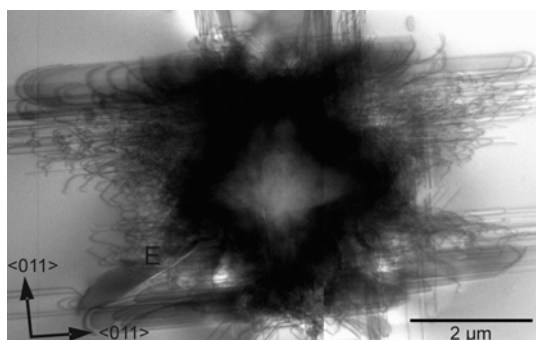


Figure 10 Multiple-beam bright-field TEM image: E-crack at a Vickers indentation in GaAs:Te, load: 0.04 N. The distinction between the $[011]$ and $[0\bar{1}1]$ directions has not been made.

E-cracks emanate like A-cracks and B-cracks from a region of high dislocation density. In TEM plane view images, the crack nucleation site is not visible due to the indentation and the high dislocation density around it. In contrary to A-cracks and B-cracks, E-cracks cut one arm of surface parallel dislocations (Fig. 10), and their strain fields may strongly interact.

5 Conclusions In the investigations of dislocations and crack patterns, no straightforward correlation between the anisotropy of the dislocation rosette, resulting from the different velocities of α and β dislocations, and the crack pattern anisotropy could be identified in (100) GaAs wafers with different dopants. The anisotropy of dislocation velocities led to the formation of slip lines in the direction of dislocations having the higher velocity. In GaAs doped with carbon, tellurium or silicon, slip lines ran parallel to the $\pm [011]$ directions. In zinc-doped GaAs, they were parallel to $\pm [0\bar{1}1]$. In GaAs:C, there is a distinct anisotropy of crack formation, that could be in relation to the different dislocation velocities. However, there are also anisotropic dislocation velocities in GaAs:Te, GaAs:Si and GaAs:Zn, but there is a much lower or no anisotropy in crack formation.

The scattering of the number of cracks formed is high. In future experiments, it may be reduced by an improved control of the loading and unloading rate and higher statistics. Additionally, the role of the shape of the indenter used in the experiment should be considered.

In CL investigations, dislocation half loops running parallel to the surface can be well observed. There were no dislocations visible near the crack tips. TEM plane view images showed that A-cracks and B-cracks pass through the region between two surface parallel dislocation branches without interaction. Hence, these dislocations do not participate in the crack formation and propagation. There are no systematic differences of dislocations with respect to the formation of A-, B- and E-crack formation in different directions. All types of cracks emanate from a region with a high dislocation density near the indentation.

The question, why there is a distinct anisotropy in the crack pattern for carbon-doped GaAs in a certain load rate could not yet be answered conclusively. The anisotropy in dislocation pattern may be ruled out. In GaAs doped with silicon, tellurium or zinc having a distinct anisotropy in the dislocation mobility, no clear anisotropy in the crack pattern could be found. Probably, there is a multitude of factors influencing the crack formation and propagation. Post mortem experiments, like the presented ones, can hardly separate the factors leading to crack formation – like the generation of dislocation barriers – or the control of crack propagation – like interaction with the strain field of dislocations, direction depending lattice trapping etc. In order to observe Lomer-Cottrell dislocations and the crack seeds, cross section TEM investigations of the region beneath the indentation would be required. In situ CL studies of indentation experiments could provide further information about the propagation of cracks and dislocations.

Acknowledgements The authors would like to thank Freiburger Compound Materials GmbH for supplying GaAs Wafers. Parts of the indentation experiments have been carried out in the group of Prof. M. Schaper (Technische Universität Dresden).

References

- [1] K. Sumino, in: Handbook of Semiconductors, Vol. 3A, edited by S. Mahajan (Elsevier Science B.V., 1994), p. 73.
- [2] G. Lu and D. J. H. Cockayne, *Physica B* **116**, 646 (1983).
- [3] J. Bohm, *Realstruktur von Kristallen* (E. Schweizerbart'sche Verlagsbuchhandlung, 1995), pp. 257/258.
- [4] S. Fujita, K. Maeda, and S. Hyodo, *Phys. Status Solidi A* **109**, 383 (1988).
- [5] P. D. Warren, P. Pirouz, and S. G. Roberts, *Philos. Mag. A* **50**, L23 (1984).
- [6] R. W. Margevicius and P. Gumbsch, *Philos. Mag. A* **78**, 567 (1998).
- [7] T. Zhu, J. Li, and S. Yip, *Proc. Roy. Soc. A* **462**, 1741 (2006).
- [8] F. Bergner, U. Bergmann, M. Schaper, R. Hammer, and M. Jurisch, *Materialprüfung* **43**, 117 (2001).
- [9] F. Bergner, M. Schaper, R. Hammer, M. Jurisch, A. Kleinwächter, and T. Chudoba, *Int. J. Mater. Res.* **97**, 735 (2007).